Published by
NIGERIAN SOCIETY OF PHYSICAL SCIENCES
Available online @ https://asr.nsps.org.ng/index.php/asr

African Scientific Reports 4 (2025) 329

African Scientific Reports

Application of modified analytical embedded atom method to the study of lattice vibration in bcc transitional metals

Akpata Erhieyovwe[a,*], Ernest Ojegu[a], Aroghene Edison Enaibe[b]

[a]*Department of Physics, Delta State University, Abraka, Delta State Nigeria*
[b]*Department of Physics, Federal University of Petroleum Resources, Effurun, Delta State, Nigeria*

Abstract

The phonon dispersion curve of four bcc transition metals - (Fe), (W), (Mo), and (Cr) - along the principal symmetry [1,0,0], [1,1,1], and [1,1,0] of the Brillouin Zone (BZ) up to the second nearest neighbors is reproduced using the Modified Analytical Embedded Atom Method (MAEAM) in conjunction with the theory of lattice dynamics. The results obtained are consistent with experimental results, and for all the bcc transition metals taken into consideration, the force constants generated with the MAEAM indicate that the force constants corresponding to the second nearest neighbors were less than the force constants corresponding to the first nearest neighbors. Additionally, the elements of the force constant matrix along ϕ_{xy}, ϕ_{xz}, and ϕ_{yz} are all zero (0). All of the resulting dynamical matrices are diagonal. The generated dispersion curves correlate well with the experimentally generated ones. This demonstrates that the MAEAM is a very effective method for researching the lattice dynamics in bcc transition metals when combined with the theory of lattice dynamics.

DOI:10.46481/asr.2025.4.3.329

Keywords: Transition metal, Lattice dynamics, Nearest neighbour, Modified analytical embedded atom method, Force constant matrix

Article History :
Received: 03 June 2025
Received in revised form: 18 August 2025
Accepted for publication: 22 August 2025
Published: 07 September 2025

1. Introduction

Metals are solids with a high electrical conductivity and a large number of mobile electrons. The valence electrons of the atom are the conduction electrons in metals. The abundance of comparatively weakly bound electrons is a defining characteristic of metallic crystals. The primary feature of a metallic bond is the decrease in the energy of the valence electrons in the metal relative to the free atom.

Phonon dispersion is the general term used to describe the lattice properties that reveal the peculiarities of the interatomic interactions in crystals. Numerous crucial details regarding the physical characteristics of solid materials, including specific heat, heat conduction, sound speed, resistivity, superconductivity, optical and magnetic properties, etc., are provided by the phonon dispersion relation. Applying experimental research of the lattice dynamics in conjunction with theoretical analysis is the most effective method for studying interatomic forces, electron phonon interaction, and related phenomena.

In a rigid crystal lattice, like the atomic lattice of a solid, phonons are a quantized mode of vibration. It is impossible to overstate the significance of phonon research for science and technology. Since the majority of a solid's physical characteristics, including its

*Corresponding author: Tel. No.: +234-802-451-5959.
Email address: erhieyovwe.akpata@delsu.edu.ng (Akpata Erhieyovwe)

electrical conductivity, magnetic properties, optical properties, and thermal conductivity, are largely determined by the behavior of its lattice dynamics, phonon research is a crucial aspect of solid state physics.

Theoretical and experimental studies of the phonon dispersion relation of materials have been conducted recently. The inelastic neutron scattering method has been successfully used to measure the phonon dispersion relation of solids because of advancements in diamond-anvil techniques and the expansion of the range for X-ray measurements under static pressure [1, 2].

Because it gives precise information about the atomic interaction, first principle calculation is a good method of determining phonon dispersion relation of solids. To get the results, the method needs a lot of time and processing power. These factors have led to the development of certain empirical many-body techniques for studying the physical characteristics of solids [3, 4]. The Embedded Atom Method (EAM) [5] is one of the empirical many-body models that have been extensively utilized in computer simulation studies of different defects based on the quasi atom concept and density functional theory (DFT). Each atom's energy in the EAM is calculated using the energy required to embed it in the local electron density. There are no ambiguities in this method because this density is clearly defined in the alloy and at the surfaces. Once more, the computational effort required to evaluate the EAM energy is comparable to that of simple pair potentials. Large-scale computer simulations of a wide range of phenomena are therefore still possible. Therefore, the EAM offers a very novel method for calculating metallic systems atomistically. Condensed matter issues such as bulk properties, grain boundaries, surfaces, and alloys have been effectively addressed by the EAM since its inception [6].

Notwithstanding the EAM's many benefits over first principle and pair potential approaches, it has certain drawbacks. For example, the atomic density (ρ) was not determined analytically; rather, it was fitted from the atomic electron density [7], and that the spherically averaged density in free electrons differs from the bulk density. This renders the computation untrustworthy. There are too many parameters in the EAM to be decided upon during computation. These consist of the following: scaling factor for embedding energy (A), equilibrium nearest neighbor distance (r_e), cohesive energy Ec (eV), weighting decay factor for atomic densities $t^{(l)}$, exponential decay factor for atomic density $\beta^{(P)}$, and density scaling factor ρ_{ao}. A first neighbor central potential model for the diamond structure is $C_{11} = C_{22}$ [8]. However, silicon doesn't meet this requirement. For silicon, F"(ρ) is negative, which deviates from the EAM requirement that $C_{12} - C_{44} > 0$. Because of these and other limitations shown by the EAM and the need to have better results, different researchers have modified the EAM visa a viz Modified Embedded Atom Method (MAEM), Analytical Embedded Atom Method (AEAM), Analytical Modified Embedded Atom Method (AMEAM) and recently the Modified Analytical Embedded Atom Method (MAEAM) [9].

Thus far, the Modified Analytical Embedded Atom Method (MAEAM) has produced better results than all other EAM modifications. In order to reproduce the phonon frequency of certain bcc transition metals, we employed the Modified Analytical Embedded Atom Method (MAEAM), the Universal form of the embedding function, and the theory of lattice dynamics.

In preparing this manuscript, we sectioned it into introduction, mathematical techniques, results, results discussion, and conclusion.

2. Mathematical theory and methodology

2.1. The basic equations of the MAEAM

The total energy of a system E_t is determined using the modified analytical embedded atom method approach of [10, 11]:

$$E_t = \sum_i F(\rho_i) + \frac{1}{2}\sum_{i\neq j}\phi(r_{ij}) + \sum_i M(P_i), \tag{1}$$

where r_{ij} is the distance between atoms i and j, $\phi(r_{ij})$ is the interaction pair potential between atoms i and j, $M(P_i)$ is the modified term, and $F(\rho_i)$ is the energy to embed an atom in site i with electron density ρ_i, which is determined by a linear superposition of the spherical averaged atomic electron density of the other atoms. It explains the energy shift brought on by the non-spherical electron (P_i) distribution and the departure from the linear superposition of the crystal's atomic electron density.

The following is the format of the modified term, pair potential, and embedding function [6]:

$$M(P_i) = \alpha \sum_i \left(\frac{P_i}{P_{ie}} \ln\left(\frac{P_i}{P_{ie}}\right)\right), \tag{2}$$

$$\phi(r) = \frac{K_0}{(r_{ie}/r)^m} + \frac{K_1}{(r_{ie}/r)^n} + \frac{K_2}{(r_{ie}/r)^k} + \frac{K_3}{(r_{ie}/r)^l}, \tag{3}$$

$$F(\rho_i) = -F_0\left[1 - \ln\left(\frac{\rho_i}{\rho_e}\right)^n\right]\left(\frac{\rho_i}{\rho_e}\right)^n. \tag{4}$$

Table 1: Input parameters for bcc transition metals [9].

Metal	a (nm)	Ω (nm^3)	E_c (eV)	E_{if} (eV)	C_{11} (GPa)	C_{12} (GPa)	C_{44} (GPa)
Iron	0.28664	0.011776	4.2800	1.7900	1440	840	730
Tungsten	0.3165	0.015852	8.9000	3.9500	3230	1270	980
Molybdenum	0.31468	0.01558	6.8200	3.1000	2870	1050	690
Chromium	0.28846	0.012001	4.1000	1.600	2160	410	620

In this work, we employed the universal form of the embedding function while our cut-off radius of interaction potential (r_{ce}) for the bcc transition metals were chosen to reside between the first and second nearest neighbours:

$$\rho_i = \sum_{j\neq i} f(r_{ij}), \tag{5}$$

$$f(r) = f_e \exp\left[-\beta\left(\frac{r}{r_{ie}} - 1\right)\right], \tag{6}$$

and r_{ie} is the nearest neighbour distance at equilibrium. For bcc lattice, it is obtained using:

$$r_{ie} = \frac{\sqrt{3}}{2}a. \tag{7}$$

Equations (8) to (15) which are the input parameters, were taken as constants in using the MAEAM to calculate the total energy of a system:

$$F_0 = E_c - E_{if}, \tag{8}$$

where E_C is cohesive energy while E_{if} is the mono-vacancy formation energy.

$$n = \frac{\Omega(C_{11} + 2C_{12})}{9B\Omega - (E_c - E_{if})}, \tag{9}$$

$$\alpha = \frac{9B\Omega - (E_c - E_{if})}{6}, \tag{10}$$

$$K_0 = -\frac{(E_c - E_{if}) + 9B\Omega(n-1)}{6}, \tag{11}$$

$f_e = 1$ for bcc transition metals [12] and

$$K_1 = \frac{\Omega}{12}\left[(C_{11} - C_{12} - 4C_{44})\left(\frac{r_{ie}}{r_{2e}}\right)^2 + 8C_{44}\left(\frac{r_{ie}}{r_{1e}}\right)^2\right], \tag{12}$$

$$K_2 = \frac{\Omega}{12}\left[(C_{11} - C_{12} - 4C_{44})\left(\frac{r_{ie}}{r_{2e}}\right)^2 + 8C_{44}\left(\frac{r_{ie}}{r_{1e}}\right)^2\right], \tag{13}$$

$$K_3 = \frac{\Omega}{12}\left[(C_{11} - C_{12} - 4C_{44})\left(\frac{r_{ie}}{r_{2e}}\right)^2 + 8C_{44}\left(\frac{r_{ie}}{r_{1e}}\right)^2\right], \tag{14}$$

$$\beta = \sqrt{\frac{9B\Omega}{E_c - E_{if}}}, \tag{15}$$

$$P_i = \sum_{j\neq i} f^2(r_{ij}), \tag{16}$$

where a is the lattice constant, $\Omega = a^3/2$, the atomic volume, and C_{11}, C_{12}, and C_{44} are the elastic constants of the bcc transition metals under consideration [14]. The computed constants for the total energy were obtained by using equations (8) to (16). Table 1 shows the input parameters for bcc transition metals.

Table 2: Coordinates of atomic positions with respect to a given origin of the bcc lattice [13].

S/N	Origin of Coordinates	1st Nearest Neighbours to the atom at the origin.	2nd Nearest Neighbours to the atom at the origin.
1	$\frac{a}{2}$(0,0,0)	$\frac{a}{2}$(1,1,1)	$\frac{a}{2}$(2,0,0)
2		$\frac{a}{2}$(1,1,-1)	$\frac{a}{2}$(-2,0,0)
3		$\frac{a}{2}$(1,-1,1)	$\frac{a}{2}$(0,2,0)
4		$\frac{a}{2}$(1,-1,-1)	$\frac{a}{2}$(0,-2,0)
5		$\frac{a}{2}$(-1,1,1)	$\frac{a}{2}$(0,0,2)
6		$\frac{a}{2}$(-1,1,-1)	$\frac{a}{2}$(0,0,-2)
7		$\frac{a}{2}$(-1,-1,1)	
8		$\frac{a}{2}$(-1,-1,-1)	

2.2. Phonon force constant model

Every nearest neighbor atom closest to the reference atom is given a force constant matrix in order to analytically determine the lattice dynamics or phonons for a particular crystal structure. By analyzing the second derivatives of the total energy E_t of a system of atoms using equation (1) with respect to the atom coordinates, the atomic force constant was determined using the modified analytical embedded atom method, a semi-empirical approach. That is:

$$\Phi_{\alpha\beta}(ij) = \frac{\partial^2 E_t}{\partial u_i^\alpha \partial u_j^\beta}. \tag{17}$$

Equation (1) was inserted into equation (17) to derive the corresponding atomic force constants, which result in [1]:

$$\begin{aligned}
\Phi_{\alpha\beta}(ij) = &\left[\phi''(r_{ij}) - \frac{\phi'(r_{ij})}{r_{ij}}\right]\frac{r_{ij}^\alpha r_{ij}^\beta}{r_{ij}^2} + \frac{\phi'(r_{ij})}{r_{ij}}\delta_{\alpha\beta} \\
&+ \left(F''(\rho_i) + F''(\rho_j)\right) f'(r_{ij}) f'(r_{ij}) \frac{r_{ij}^\alpha r_{ij}^\beta}{r_{ij}^2} \\
&+ F'(\rho_i) f''(r_{ij}) \frac{r_{ij}^\alpha r_{ij}^\beta}{r_{ij}^2} + F'(\rho_i)\frac{f'(r_{ij})}{r_{ij}}\left(\delta_{\alpha\beta} - \frac{r_{ij}^\alpha r_{ij}^\beta}{r_{ij}^2}\right) \\
&+ \delta_{ij}\sum_{k\neq i}\left(F''(\rho_i) f'(r_{ik}) f'(r_{ik}) \frac{r_{ik}^\alpha r_{ik}^\beta}{r_{ik}^2} + F'(\rho_i) f''(r_{ik}) \frac{r_{ik}^\alpha r_{ik}^\beta}{r_{ik}^2} + F'(\rho_i)\frac{f'(r_{ik})}{r_{ik}}\left(\delta_{\alpha\beta} - \frac{r_{ik}^\alpha r_{ik}^\beta}{r_{ik}^2}\right)\right) \\
&+ \left(M''(P_i) + M''(P_j)\right) g'(r_{ij}) g'(r_{ij}) \frac{r_{ij}^\alpha r_{ij}^\beta}{r_{ij}^2} + M'(P_i) g''(r_{ij}) \frac{r_{ij}^\alpha r_{ij}^\beta}{r_{ij}^2} + M'(P_i)\frac{g'(r_{ij})}{r_{ij}}\left(\delta_{\alpha\beta} - \frac{r_{ij}^\alpha r_{ij}^\beta}{r_{ij}^2}\right) \\
&+ \delta_{ij}\sum_{k\neq i}\left(M''(P_i) g'(r_{ik}) g'(r_{ik}) \frac{r_{ik}^\alpha r_{ik}^\beta}{r_{ik}^2} + M'(P_i) g''(r_{ik}) \frac{r_{ik}^\alpha r_{ik}^\beta}{r_{ik}^2} + M'(P_i)\frac{g'(r_{ik})}{r_{ik}}\left(\delta_{\alpha\beta} - \frac{r_{ik}^\alpha r_{ik}^\beta}{r_{ik}^2}\right)\right),
\end{aligned} \tag{18}$$

where ($'$) and ($''$) are the first and second derivatives respectively, $\delta_{\alpha\beta}$ is one if $\alpha = \beta$ and zero otherwise, α and β refers to Cartesian coordinates and r_{ij}^α r_{ij}^β r_{ik}^α and r_{jk}^β are unit vectors.

Only the first neighbor interaction pair potential ϕ was taken into account when calculating the atomic force constant using equation (17), but the modified terms M(P) and the embedding functions F(ρ) for each of the nearest neighbors were taken into account. We assumed in our computation that the atoms in the host crystals that are not the second neighbors are undisturbed. The force constant matrix for the first and second nearest neighbors was created using equation (18).

2.3. Dynamical matrix calculation

In constructing the dynamical matrix, we assigned a force constant to every atom of the nearest neighbour atom to the reference atom. The expression for the dynamical matrix is taken as [15]:

$$D_{\alpha\beta}(\vec{q}) = \frac{1}{\sqrt{M_i M_j}}\sum_l \Phi_{\alpha\beta}(lj) e^{i\vec{q}\cdot(\vec{r}_l - \vec{r}_j)}. \tag{19}$$

Table 3: Calculated model parameters for the bcc transition metals.

Metals	F_0	Ω (nm^{-3})	n	α	K_0	K_1	K_2	K_3
Iron	2.49	0.011776	0.279466	-0.02428	-0.2562	-0.000197	0.001767	0.000635
Tungsten	4.95	0.015852	0.463045	-0.13258	-0.5514	-0.002587	0.01212	0.000722
Molybdenum	3.72	0.015580	0.552294	-0.14173	-0.4288	-0.002626	0.01173	0.00034
Chromium	2.5	0.012001	0.540453	-0.09133	-0.2178	-0.001985	0.00879	0.000203

Table 4: Calculated force constants $\Phi_{\alpha\beta}$ for the four bcc transition metals for 1NN to 2NN.

Metal	Nearest Neighbours	Φ_{xx} (N/m)	Φ_{yy} (N/m)	Φ_{zz} (N/m)	Φ_{xy} (N/m)	Φ_{xz} (N/m)	Φ_{yz} (N/m)
Fe	1NN	295534.0743	295534.0743	295534.0743	295534.3062	295534.3062	295534.3062
	2NN	725227578.4	-23188098	-0.23188098	0	0	0
W	1NN	141593.9406	141593.9406	141593.9406	141594.0125	141594.0125	141594.0125
	2NN	358296625.6	-0.0719054	-0.07190541	0	0	0
Mo	1NN	105746.6799	105746.6799	105746.6799	105747.2959	105747.2959	105747.2959
	2NN	265.309400.8	-0.61603476	-0.61603476	0	0	0
Cr	1NN	199825.3023	199825.3023	199825.3023	199825.8412	199825.8412	199825.8412
	2NN	496462110.2	-0.53890638	-0.53890638	0	0	0

Table 5: Force constant matrix ($\Phi_{\alpha\beta}$ (i-j)) generated for the four bcc transition metals corresponding to the first (1NN) and second 2NN neighbours of the atom at the origin ($j = 1, 2, 3 \ldots, 14$).

Atom Pair	$\Phi_{\alpha\beta}$ (i-j)	Atom Pair	$\Phi_{\alpha\beta}$ (i-j)	Atom Pair	$\Phi_{\alpha\beta}$ (i-j)
0-1	$\begin{bmatrix} A & 0 & 0 \\ 0 & A & 0 \\ 0 & 0 & A \end{bmatrix}$	0-2	$\begin{bmatrix} A & 0 & 0 \\ 0 & A & 0 \\ 0 & 0 & A \end{bmatrix}$	0-3	$\begin{bmatrix} A & 0 & 0 \\ 0 & A & 0 \\ 0 & 0 & A \end{bmatrix}$
0-4	$\begin{bmatrix} A & 0 & 0 \\ 0 & A & 0 \\ 0 & 0 & A \end{bmatrix}$	0-5	$\begin{bmatrix} A & 0 & 0 \\ 0 & A & 0 \\ 0 & 0 & A \end{bmatrix}$	0-6	$\begin{bmatrix} A & 0 & 0 \\ 0 & A & 0 \\ 0 & 0 & A \end{bmatrix}$
0-9	$\begin{bmatrix} B & 0 & 0 \\ 0 & C & 0 \\ 0 & 0 & C \end{bmatrix}$	0-10	$\begin{bmatrix} B & 0 & 0 \\ 0 & C & 0 \\ 0 & 0 & C \end{bmatrix}$	0-11	$\begin{bmatrix} B & 0 & 0 \\ 0 & C & 0 \\ 0 & 0 & C \end{bmatrix}$
0-12	$\begin{bmatrix} B & 0 & 0 \\ 0 & C & 0 \\ 0 & 0 & C \end{bmatrix}$	0-13	$\begin{bmatrix} B & 0 & 0 \\ 0 & C & 0 \\ 0 & 0 & C \end{bmatrix}$	0-14	$\begin{bmatrix} B & 0 & 0 \\ 0 & C & 0 \\ 0 & 0 & C \end{bmatrix}$

For bcc monatomic transition metals, $M_i = M_j = M$ so that equation (19) becomes:

$$D_{\alpha\beta}(\vec{q}) = \frac{1}{M} \sum_{l} \Phi_{\alpha\beta}(lj) e^{i\vec{q}\cdot(\vec{r}_l - \vec{r}_j)}. \tag{20}$$

In setting the dynamical matrix for the bcc structure in this research work, we assumed that the interatomic forces are negligible beyond the second nearest neighbours. The first to the second atomic nearest neighbours and their various coordination numbers is shown in Table 2. To get the phonon dispersion curve of the crystal, we plotted the eigenvalues (frequency ω) obtained from the dynamical matrix against the wave vectors (k).

3. Results

The input parameters and the calculated parameters for the Modified Analytical Embedded Atom Method using equations (1) to (16) are presented in Tables 1 and 3, respectively.

4. Discussion of results

Using the Modified Analytical Embedded Atom Method of [16], this study aims to obtain force constants that will be used to create a dynamical matrix. After diagonalizing the dynamical matrix, the dispersion curve was obtained by plotting the eigenvalues

Table 6: Calculated dynamical matrix elements ($D_{\alpha\beta}(\vec{q})$) for the four bcc transition metal for 1NN to 2NN.

bcc Metal	NN	Dxx(q)	Dyy(q)	Dzz(q)	Dxy(q)	Dxz(q)	Dyz(q)
Iron (Fe)	1NN	0.084668521	0.084668521	0.084668521	0	0	0
	2NN	-0.00129859	-0.00129859	23320.09829	0	0	0
Tungsten (W)	1NN	979.1071673	979.1071673	979.1071673	0	0	0
	2NN	-0.000739	-0.000739	2311430.85	0	0	0
Molybdenum (Mo)	1NN	1876.335285	1876.335285	1876.335285	0	0	0
	2NN	-0.0014162	-0.0014162	4429157.93	0	0	0
Chromium (Cr)	1NN	3462.098258	3462.098258	3462.098258	0	0	0
	2NN	-0.002613	-0.002613	8172409.58	0	0	0

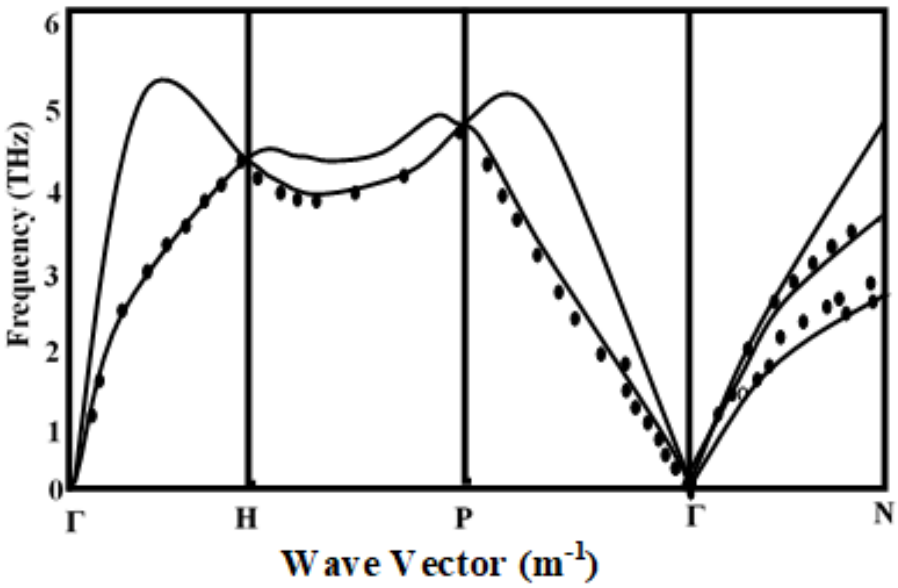

Figure 1: Phonon dispersion curve for Fe along [1,0,0], [1,1,1] and [1,1,0] directions: MAEAM and experiment [15].

against the wave vectors. The force constant generated using the MAEAM is displayed in Table 4, the force constant matrix is tabulated in Table 5, and the dynamical matrix elements produced are shown in Table 6. All the off diagonal elements of the dynamical matrix generated using the MAEAM are zero (0). This demonstrates that all the metal's dynamical matrices are diagonal.

Similar to this, the phonon dispersion curves of the bcc transition metals Fe, W, Mo, and Cr along the high symmetry directions [1,0,0], [1,1,1], and [1,1,0] have been computationally and analytically replicated using the Microsoft Excel spreadsheet up to the second nearest neighbors using the MAEAM, and the results have been compared with experimental findings.

The peculiar spots on the bcc lattice's first Brillouin zone are denoted by the letters Γ, H, P, and N. Figures 1 to 4 show the dispersion curve using the MAEAM and experimental results for the bcc metals. The eigenvalues derived from diagonalizing the dynamical matrix are responsible for the many branches of the phonon band structure that are observed. There are two branches of dispersion (Acoustic Transverse (T) and Acoustic Longitudinal (L)), according to the frequency values measured along the point of high symmetry directions (Γ →H, H→P, and P → Γ). After that, a degeneration of the Acoustic transverse branch caused the two branches to break into three branches along the Γ →N direction.

The majority of the phonon dispersion curves derived by MAEAM are consistent with those acquired by experiment. This work has somewhat reduced the anomalies between the determined and experimental values, in spite of the fact that phonon dispersion curves of bcc metals are full of anomalies [16].

5. Conclusion

Using the Modified Analytical Embedded Atom Method (MAEAM) in conjunction with the theory of lattice dynamics, the force constants and the dynamic matrix for the bcc transition metals (Fe, W, Mo, and Cr) have been successfully generated up to the second nearest neighbors (2NN). The phonon dispersion was calculated along the Brillouin Zone's (BZ) primary symmetry points

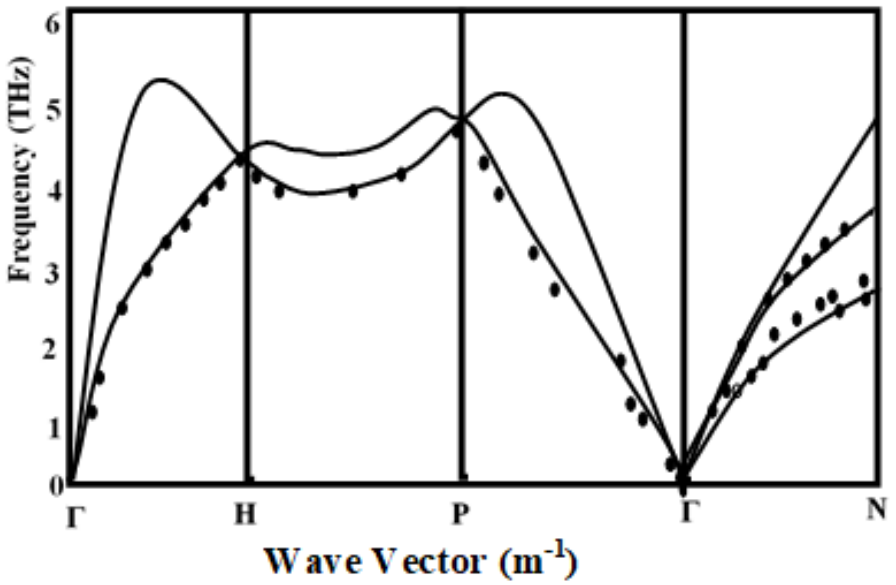

Figure 2: Phonon dispersion curve for W along [1,0,0], [1,1,1] and [1,1,0] directions: MAEAM and experiment [15].

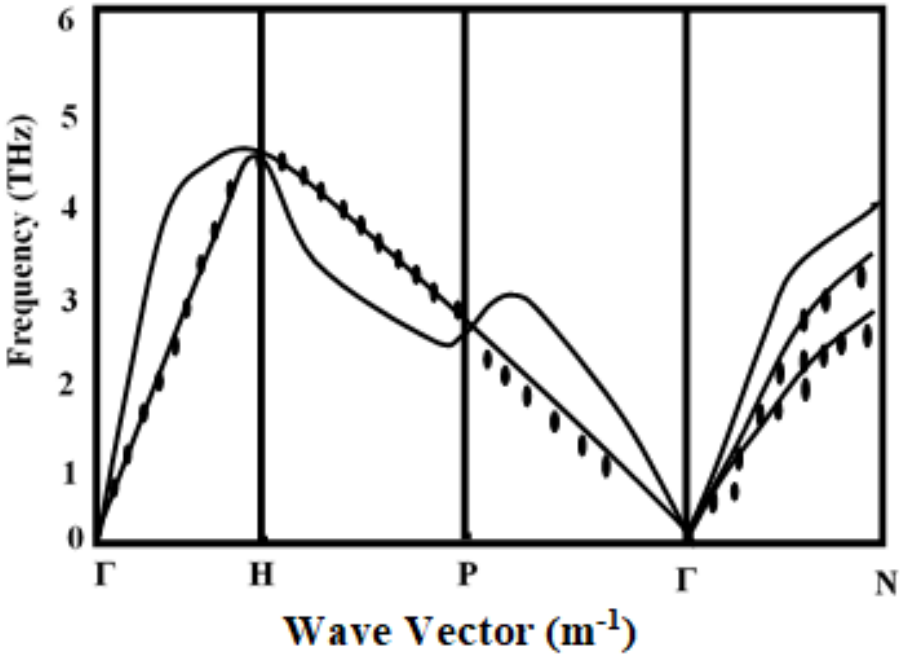

Figure 3: Phonon dispersion curves of Mo along [100], [111] and [110] directions: MAEAM and experiment [15].

and compared to the experiment's findings. The experiment's results and the dispersion curves generated by the MAEAN agree well. Thus, we conclude that the MAEAM is another potent tool that can be utilized to reproduce bcc transition metals phonon dispersion curves that are equivalent to experimental data when combined with the theory of lattice dynamics.

Data availability

Data will be made available upon reasonable request from the corresponding author.

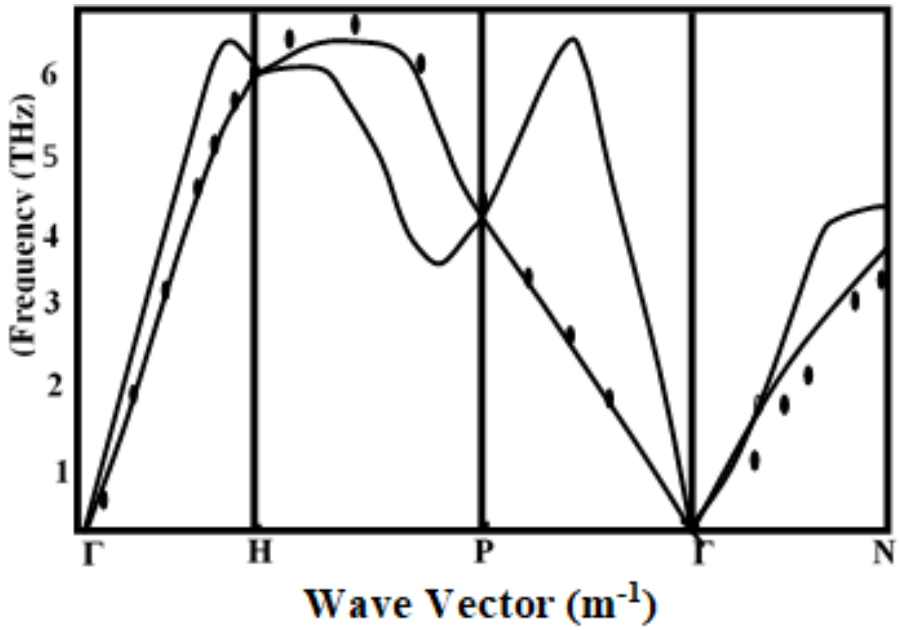

Figure 4: Phonon dispersion curves of Cr along [100], [111] and [1,1,0] direction: MAEAM, experiment [15].

Acknowledgment

The authors would like to acknowledge the Tertiary Education Trust Fund (TETfund) of the Federal Republic of Nigeria (DELSU/TETFIBR/19-23/B8/SN.3) for providing financial support for this research work.

References

[1] G. Vandana, P. D. Semalty & P. Ram, "Vibrational properties of vacancy in bcc transition metals using embedded atom method potential", Pramana J. Phys. **80** (2013) 1041. https://doi.org/10.1007/s12043-013-0539-y.
[2] O. G. Okocha, *Phonon dispersion of some bcc metals*, Ph.D. dissertation, Department of Physics, University of Benin, Benin City, Edo State, 2019.
[3] M. I. Baske, "Application of embedded-atom method to covalent materials: A semiempirical potential for silicon", Phys. Rev. Lett. **59** (1987) 2666. https://doi.org/10.1103/PhysRevLett.59.2666.
[4] M. W. Finnis & J. E. Sinclair, "A simple empirical N-body potential for transition metals", Phil. Mag. **50** (1984) 45. https://doi.org/10.1080/01418618408244210.
[5] M. S. Daw & M. I. Baske, "Semiempirical, quantum mechanical calculation of hydrogen embrittlement in metals", Phys. Rev. Lett. **50** (1983) 1285. https://doi.org/10.1103/PhysRevLett.50.1285.
[6] E. Akpata, A. E. Enaibe & A. Iyoha, "Surface energy calculation of low index group 1 alkali metals of the periodic table using the modified analytical embedded atom method", Int. J. Sci. Res. Eng. Technol. **3** (2014) 876. https://doi.org/10.18488/journal.75/2014.1.1/75.1.34.41.
[7] E. Clementi & C. Roetti, "Roothaan-Hartree-Fock atomic wavefunctions: Basis functions and their coefficients for ground and certain excited states of neutral and ionized atoms, $Z \leq 54$", At. Data Nucl. Data Tables **14** (1974) 177. https://doi.org/10.1016/S0092-640X(74)80016-1.
[8] M. S. Daw & M. I. Baske, "Embedded-atom method: Derivation and application to impurities, surfaces, and other defects in metals", Phys. Rev. B **29** (1984) 6443. https://doi.org/10.1103/PhysRevB.29.6443.
[9] E. Akpata, A. E. Enaibe & S. E. Iyayi, "Comparison of surface energy of bcc alkali metals and transitions using MAEAM", Rev. Adv. Phys. Theor. Appl. **1** (2014) 34. http://dx.doi.org/10.18488/journal.75/2014.1.1/75.1.34.41
[10] W. Y. Hu, B. W. Zhang, S. L. Shu & B. Y. Huang, "Surface energy calculation of the bcc metals using MAEAM", J. Alloys Compd. **287** (1999) 159. https://doi.org/10.1016/S0925-8388(99)00043-3.
[11] Y. Ouyang, B. Zhang, S. Liao, Z. Jin & H. Chen, "Formation enthalpies for FCC metal based binary alloys by embedded atom method", Trans. Nonferrous Met. Soc. China **8** (1998) 60. http://www.ysxbcn.com/paper/paperview.aspx?id=paper_15132.
[12] W. Y. Hu, X. L. Shu & B. W. Zhang, "Point-defect properties in bcc transition metals with AEAM interatomic potentials", Comput. Mater. Sci. **23** (2002) 175. https://doi.org/10.1016/S0927-0256(01)00238-5.
[13] Y. Nakagawa & A. D. B. Wood, "Lattice dynamics of niobium", Phys. Rev. Lett. **11** (1963) 271. https://doi.org/10.1103/PhysRevLett.11.271.
[14] X. You, J. M. Zhang & V. Ji, "MAEAM for phonon dispersion of noble metals in symmetry and off symmetry directions", Solid State Commun. **145** (2008) 182. https://doi.org/10.1016/j.ssc.2007.10.028.
[15] G. Venkataraman, L. A. Feldkamp & V. C. Sahni, *Dynamics of perfect crystals*, MIT Press, Cambridge, USA, 1975. https://mitpress.mit.edu/9780262220194/dynamics-of-perfect-crystals/.
[16] A. Verman, M. Verma & R. P. S. Rathore, "Elastic behavior and lattice vibration in bcc V and Nb", Acta Phys. Pol. A **90** (1996) 547. http://dx.doi.org/10.12693/APhysPolA.90.547.